

A natural long-term annealing experiment for the zircon fission track system in the Songpan-Garzê flysch, China

Meinert Rahn¹  | Hejing Wang² | István Dunkl³

¹Section on Geological Disposal, Swiss Federal Nuclear Safety Inspectorate, Brugg, Switzerland

²School of Earth and Space Sciences, Peking University, Beijing, China

³Geoscience Center, University of Göttingen, Göttingen, Germany

Correspondence

Dr. Meinert Rahn, Section on Geological Disposal, Swiss Federal Nuclear Safety Inspectorate, Industriestrasse 19, CH - 5200 Brugg, Switzerland.
Email: meinert.rahm@ensi.ch

Funding information

National Natural Science Foundation of China, Grant/Award Number: 40972038, 40572032 and 40872034

Abstract

Application of the zircon fission track (FT) method to derive reliable cooling histories requires that rocks have undergone temperatures sufficient to reach full resetting prior to cooling. Zircons commonly show significant variation in accumulated radiation damage and therefore FT annealing behaviour. Twenty-eight samples of mainly anchizonal to lowermost greenschist facies Triassic sandstones from the Songpan-Garzê flysch, China, were evaluated for their FT annealing status. Literature data suggest a heating period in the range of 100 myr duration. Our results define a temperature range for partial FT annealing of 270–350°C (based on illite crystallinity data), higher than the proposed range for radiation-damaged zircons. We suggest that the long residence at high temperature has led to annealing of relevant parts of radiation damage along with FT annealing, so that even for long durations of FT annealing, full resetting requires temperatures in the range of greenschist facies conditions typical for zero-damage zircons.

1 | INTRODUCTION

Zircon has been widely used to date geological processes. A correct interpretation of the ages relies on the knowledge of the corresponding closure temperature of the applied dating method. For the (U-Th)/He and fission track (FT) methods, it may additionally be necessary to know the temperature range (called partial retention zone for the He method and partial annealing zone, PAZ, for the FT method), in which the geochronological system changes from a totally open system (upper temperature boundary) to a totally closed system (lower temperature boundary).

For FT annealing in zircon, it has been shown that the upper and lower PAZ boundary temperatures are depending on the duration of a thermal event (e.g. Fleischer, Price, & Walker, 1965; Krishnaswami, Lal, Prabhu, & MacDougall, 1974; Tagami, Galbraith, Yamada, & Laslett, 1998; Yamada, Tagami, Nishimura, & Ito, 1995). Next to temperature, it has been suggested that the amount of accumulated radiation damage may influence track annealing (Kasuya & Naeser, 1988) and therefore shift the lower and upper boundary

of the zircon PAZ (Rahn, Brandon, Batt, & Garver, 2004; Reiners & Brandon, 2006). Comparison of the temperatures of radiation damage annealing and FT annealing in zircon (e.g. Ginster, Reiners, Nasdala, & Chanmuang, 2019; Jonckheere, Heinz, Hacker, Rafaja, & Ratschbacher, 2019) illustrate that radiation damage is a combination of several different effects annealing over a large temperature range.

In contrast to laboratory annealing experiments on homogeneous zircon grains, samples of sedimentary origin may show a large variation in uranium content and therefore radiation damage accumulated since zircon grain formation. This may lead to the situation that within a single sample zircon grains may show different annealing properties. For such a case, a χ^2 age may be calculated to separate the age information from a fully annealed grain population (Brandon, Roden-Tice, & Garver, 1998). Depending on the sample material, the χ^2 age may represent a geologically meaningful cooling age. However, without any further information apart from a statistical argument, the youngest population could still be a mixture of several populations including partially annealed material. Additional evidence, such as track length data or maximum temperature information is required to fully assess the annealing status.

This paper was presented at the 16th International Conference on Thermochronology (Quedlinburg, Germany, September 2018).

Zircon FT etching times depend on the accumulated radiation damage (Bernet & Garver, 2005). In case of sufficient material, several mounts may be prepared and different etching times applied. If the focus is on finding all grain populations (e.g. for full provenance reconstruction), several mounts may be needed to overcome heterogeneous etching properties. However, if dating tries to resolve the youngest grain population (e.g. for deriving a cooling age), etching will commonly focus on those grains with longest etching times. Such a strategy may miss the full range of detrital information, but focusses on a population that is thought to represent a cooling age. For both types of studies, however, during zircon etching a substantial fraction of embedded grains may be lost due to the faster etching observed for highly damaged zircons. Furthermore, track densities in old grain populations may often be too high or grain colour too dark (Garver and Kamp, 2002) to give reliable counting results. Old or highly damaged grains tend to be overetched and therefore not suitable for counting. We conclude that irrespective of the questions to be answered by a zircon FT study, the selection of grains suitable for counting will tend to focus on grains with low levels of radiation damage.

In this study, we report a set of 28 zircon FT data from the Songpan-Garzê flysch, whose diagenetic to metamorphic overprint has been determined recently on the basis of sheet silicate crystallinity (Wang, Rahn, Tao, Zheng, & Xu, 2008; Wang, Ma, Zhou, & Xu, 2012; Wang, Rahn, Zhou, & Tao, 2013; Wang, Rahn, & Zhou, 2018, for a summary of methodical aspects, see Data S1). For the thermal evolution of the flysch after sedimentation, a thermal plateau of 100 myr duration has been proposed (Roger, Jolivet, Cattin, & Malavieille, 2011), which allows to evaluate zircon annealing properties for a very long annealing period. Maximum temperatures reached during the thermal plateau are compared with the observed degree of annealing to determine the temperature range required from initial to full annealing.

2 | GEOLOGICAL SETTING

The Songpan-Garzê flysch was formed due to continent–continent collision between the North China, South China and Qiangtang Blocks during the Triassic Indosinian orogeny (e.g. Pullen, Kapp, Gehrels, Vervoot, & Ding, 2008). Substantial exhumation of the Qinling-Dabie orogen on the North China Block led to erosion of vast amounts of clastic material into large-scale foreland basins that existed on both sides of the collision belt (Ma, Fu, Wu, & Chen, 2007; Weislogel et al., 2006). The zircons accumulated in the flysch sandstones of the Songpan Basin south of the Qinling-Dabie orogen were mainly deposited during the Middle and Upper Triassic as deep sea turbidites (Ma, Mou, Guo, Yu, & Tan, 2006), continuously evolving into more coarse-grained clastic sediments in the Upper Triassic. Syn-sedimentary folding and faulting in an accretionary wedge setting (Roger et al., 2011), resulted in a thick crustal sequence that later was locally intruded by mainly granitoid melts since the Triassic (Chen & Arnaud, 1997; Hu, Meng, Shi, & Qu, 2005). Magmatism continued up to the Cretaceous (e.g. Roger, Malavieille, Leloup, Calassou, & Xu, 2004), and ongoing crustal thickening and shortening eventually resulted in exhumation of the crust (Roger et al., 2011; Wang et al., 2009, 2011).

Samples for this study were collected from a profile across the Longmenshan Fault in the east, which separates the Songpan-Garzê-Bayan-Har Terrane from the Sichuan Basin (around Chengdu, Figure 1), to the area along the railway track south of Golmud in the west. Several hundreds of intercalated clay layers in the flysch were analysed for their illite crystallinity (IC) to reveal the pattern of regional thermal overprint (Wang et al., 2008, 2012, 2013, 2018). IC values range from diagenesis to greenschist facies (Figure 1), with the exception of a domal structure of up to amphibolite facies in the Danba area (corresponding to the M2 metamorphic event of Huang, Maas, Buick, & Williams, 2003).

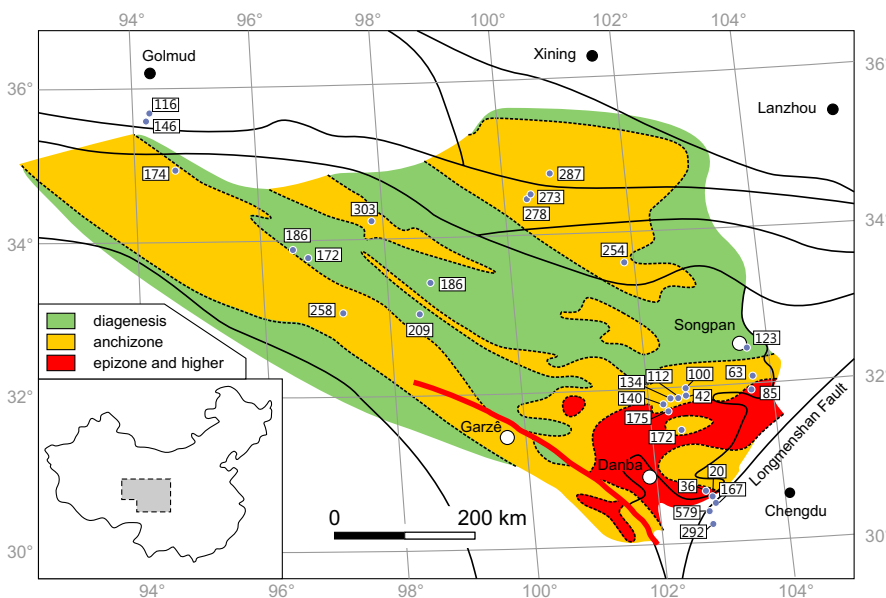


FIGURE 1 Tectonic and metamorphic map of the Songpan-Garzê-Bayan-Har Terrane with diagenetic to metamorphic zoning pattern according to Wang et al. (2008, 2013, 2018) on the basis of several hundred illite crystallinity measurements. The anchizone boundaries correspond to maximum temperatures of ~ 240 and 300°C (Mullis et al., 2018). The localities of 28 zircon fission track samples investigated for this study are marked with blue dots and their pooled age (in Ma). Black lines indicate terrane boundaries; the thick red line indicates the Xianshuihe Fault, which reveals a lateral offset in the metamorphic pattern (Wang et al., 2013)

Based on a compilation of geochronological data from several places in the study area, Roger et al. (2011) derived a cooling history with a thermal plateau lasting from the early Jurassic to the late Cretaceous, that is covering a time duration in the range of 100 myr (Figure 2). Other reconstructions have proposed an early Jurassic thermal peak, followed by continuous cooling to surface conditions (e.g. Wang et al., 2009, see Figure 2), which are at odds with geochronological evidence (e.g. Guenther, Reiners, & Tian, 2014). We here adopt that the thermal overprint in the Songpan-Garzê-Bayan-Har Terrane lasted for a time duration of 100 myr.

3 | RESULTS

Triassic flysch sandstones from the Songpan-Garzê flysch were sampled together with mostly upper anchizone to epizonal intercalated schists (Wang et al., 2008, 2012, 2013, 2018; compiled for the eastern Songpan-Garzê-Bayan-Har Terrane in Figure 1). Additional samples collected across a sample profile across the Longmenshan Fault include a granite, surrounded by greenschist facies rocks next to the fault, and unmetamorphosed sandstones of Triassic and Devonian age east of it (Sichuan Basin). IC values vary from diagenetic ($0.79 \Delta^{\circ}2\theta$) to epizone ($0.22 \Delta^{\circ}2\theta$), normalized to anchizone boundaries of 0.42 and $0.25 \Delta^{\circ}2\theta$ according to international standards (Warr

& Rice, 1994). The term 'epizone' here refers to a transitional zone between anchizone and greenschist facies. For greenschist facies rocks, an approximate minimum temperature of 350°C is assumed.

Zircons were separated using standard disaggregation and separation procedures. Mineral grains were mounted in Teflon[®], etched within a NaOH-KOH eutectic melt (Gleadow, Hurford, & Quaipe, 1976) at 220°C . Up to two mounts per sample were prepared and these mounts were etched in order to properly reveal tracks in those zircon grains of slowest etching properties. Applied etching times varied between 20 and 109 hr (see detailed etching information in the Data S1). Track counting and length measurements were carried out under oil at $2,000\times$ magnification using transmitted light.

Zircon pooled FT ages vary between 20 and 580 Ma (Table 1, Figure 3). For the data set of mainly Triassic flysch samples, such spread in ages indicates variable stages of annealing. Mean ages show two loosely defined age clusters at 240–300 Ma, representing the cooling ages from the relatively fast exhuming hinterland (detrital ages, which are contemporaneous to slightly older than the Triassic sedimentation age), and at 110–170 Ma, which cannot be directly related to any known cooling event within the Songpan-Garzê-Bayan-Har Terrane. The youngest zircon FT age of 19.8 Ma is found for the granite sample next to the Longmenshan Fault (greenschist facies), the oldest mean age (577 Ma) comes from a Devonian sandstone sample east of the Longmenshan Fault (Sichuan Basin, diagenetic).

Mean track lengths vary from 7.5 to $10.9 \mu\text{m}$, with many track length distributions being skewed towards shorter tracks (Figure 4, and data overview in Data S1). The majority of the measured tracks are TINTs (tracks in tracks, Laslett, Kendall, Gleadow, & Duddy, 1982), as cleavage cracks only occur occasionally. A relationship between mean track lengths and the angle of measurements, as observed by Yamada et al. (1995), was only observed for the sample with the shortest mean track length ($7.51 \mu\text{m}$, RW-68), for all other samples L_{60} and L_{all} are indistinguishable within uncertainty (Table 1). In a boomerang plot (Figure 3), most samples from the above-mentioned two age clusters show long mean track lengths, together with the youngest age (19.8 Ma, Figure 4). Track length distributions of the intermediate age cluster, however, are markedly skewed (see diagrams in Data S1), illustrating the presence of shortened tracks and therefore no full resetting. The age-length distribution is interpreted to show a double boomerang with the first boomerang ranging from the Triassic to the Cretaceous/Jurassic age cluster and the second from the Cretaceous/Jurassic to the reset Miocene zircon age. For the samples close to the Danba area (Figure 1), the Cretaceous/Jurassic ages may be related to the M2 metamorphic event in the southeastern flysch region (Huang et al., 2003). However, similar ages are also found near the Kunlun Fault and other faults, which may alternatively be related to the slightly younger closure of the Bangong suture zone (Figure 4, Zhu et al., 2016) causing exhumation effects in the vicinity to the major faults of the Tibetan Plateau.

In order to assess the annealing status of the different samples, a classification based on three aspects was applied: (a) the range of single grain ages with respect to the sedimentation age and the apatite FT age (if applicable), (b) the mean track length and shape of the track

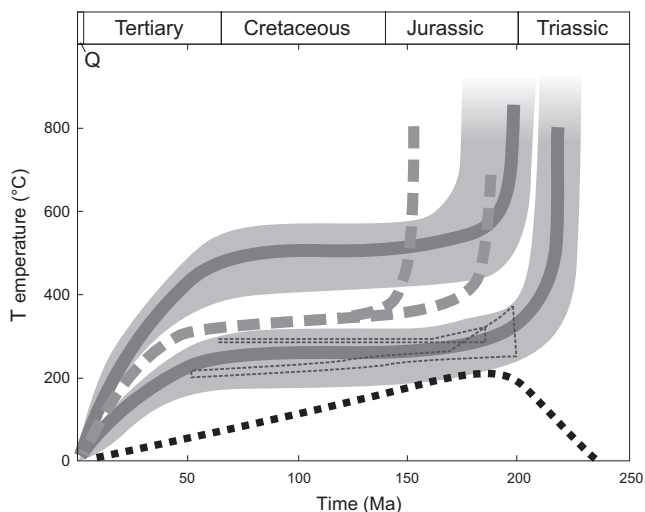


FIGURE 2 Proposed cooling histories of the Songpan-Garzê-Bayan-Har Terrane and Kunlun area, as derived mostly from geochronological data for different intrusive bodies in the terrane (light grey envelopes, thick dark grey lines and thick intermediate grey dashed lines from a compilation by Roger et al., 2011), together with polygons of thin dashed lines derived from the modelling of time-temperature evolutions by Ar/Ar thermochronology data on feldspar (Kirby et al., 2002). The derived cooling history shows magmatic cooling down to a thermal plateau, which seems to have lasted for more than 100 myr. In contrast, Wang et al. (2009) (thick black dashed line) suggested for the flysch sandstones in the Bayan-Har area (near Golmud, Figure 1) constant cooling after an initial phase of burial, which is at odds with geochronological evidence of the entire terrane. Q = Quaternary

TABLE 1 Zircon fission track (FT) data from flysch sandstones of the Songpan-Garzé-Bayan-Har Terrane, Tibetan Plateau, China

Sample no. (long/lat, in degrees, elevation in m)	Mineral and no. crystals	Spontaneous, ρ_s (N_j)	Induced, ρ_i (N_i)	$P\chi^2$ (%)	Dosimeter, ρ_d^* (N_d)	Pooled FT age (Ma) ($-2\sigma/+2\sigma$)	Mean track length	SD of distribution (No. tracks)	L_{60}
RW 010 (103.6,778/31.9,242, 1,804)	Zircon (20)	0.633 (1,469)	0.336 (779)	39	6.767 (3,889)	84.8 (-8.5/+9.4)	9.86	1.08 (85)	9.97
RW 011 (103.7,210/32.0,947, 1,805)	Zircon (20)	0.442 (742)	0.314 (527)	70	6.767 (3,889)	63.4 (-7.6/+8.6)	9.34	1.49 (75)	9.29
RW 013 (103.6,792/32.4,499, 2,439)	Zircon (20)	0.780 (2,104)	0.279 (752)	<1	6.767 (3,889)	125.4 (-12.2/+13.5)	10.09	1.35 (89)	9.96
RW 045 (102.6,327/31.9,856, 3,268)	Zircon (20)	0.494 (1,744)	0.223 (786)	64	6.768 (3,890)	99.7 (-9.8/+10.9)	9.72	1.06 (100)	9.72
RW 046 (102.6,378/31.8,904, 3,174)	Zircon (20)	0.214 (1,178)	0.228 (1,253)	36	6.769 (3,890)	42.4 (-4.0/+4.5)	9.70	1.40 (100)	9.58
RW 047 (102.5,218/31.8,527, 2,938)	Zircon (20)	0.578 (2,088)	0.232 (839)	93	6.770 (3,891)	111.7 (-10.6/+11.7)	10.43	0.83 (100)	10.44
RW 048 (102.3,835/31.8,616, 2,841)	Zircon (20)	0.589 (1,998)	0.195 (628)	2	6.770 (3,891)	135.4 (-13.9/+15.4)	10.61	0.87 (91)	10.65
RW 049 (102.2,677/31.7,918, 3,048)	Zircon (20)	0.533 (1,442)	0.163 (440)	<1	6.771 (3,892)	146.7 (-16.8/+19.0)	10.39	0.86 (100)	10.40
RW 050 (102.3,133/31.7,070, 4,027)	Zircon (20)	0.817 (2,339)	0.208 (596)	90	6.772 (3,892)	175.3 (-17.9/+19.9)	10.04	1.23 (89)	10.08
RW 052 (102.5,072/31.4,402, 3,029)	Zircon (20)	0.621 (3,064)	0.169 (831)	<1	6.773 (3,892)	164.9 (-15.2/+16.8)	10.42	1.11 (100)	10.36
RW 065 (102.7,896/30.6,425, 1,908)	Zircon (17)	0.166 (480)	0.212 (613)	9	6.773 (3,893)	35.4 (-4.4/+5.1)	9.84	1.48 (71)	9.75
RW 067 (102.8,775/30.5,768, 1,607)	Zircon (20)	0.125 (360)	0.285 (822)	80	6.773 (3,893)	19.8 (-2.6/+2.9)	10.86	0.89 (61)	10.79
RW 068 (102.8,979/30.4,930, 1,301)	Zircon (20)	1.350 (1,627)	0.242 (292)	<1	6.774 (3,893)	247.4 (-31.5/+36.0)	7.51	1.80 (40)	7.00
RW 069 (102.8,134/30.3,874, 1,094)	Zircon (20)	1.330 (2,645)	0.100 (198)	36	6.775 (3,894)	577.5 (-80.6/+93.1)	8.11	1.49 (100)	8.08
RW 072 (102.8,396/30.2,274, 784)	Zircon (20)	0.850 (4,272)	0.130 (653)	<1	6.775 (3,894)	289.7 (-27.7/+30.6)	9.83	1.34 (100)	9.70
RW 094 (101.8,837/33.6,096, 3,616)	Zircon (20)	1.110 (3,737)	0.184 (620)	<1	6.776 (3,894)	267.4 (-26.1/+28.9)	10.04	1.30 (92)	9.87
RW 127 (98.7,267/33.4,201, 4,932)	Zircon (20)	0.787 (2,334)	0.166 (491)	65	6.776 (3,895)	211.8 (-22.7/+25.3)	10.36	1.27 (82)	10.41
RW 139 (100.4,052/34.4,751, 4,212)	Zircon (20)	1.000 (2,642)	0.160 (421)	27	6.777 (3,895)	278.2 (-30.8/+34.5)	10.66	0.95 (100)	10.65

(continues)

TABLE 1 (continued)

Sample no. (long/lat. in degrees, elevation in m)	Mineral and no. crystals	Spontaneous, ρ_s (N_s)	Induced, ρ_i (N_i)	$P\chi^2$ (%)	Dosimeter, ρ_d^* (N_d)	Pooled FT age (Ma) ($-2\sigma/+2\sigma$)	Mean track length	SD of distribution (No. tracks)	L_{60}
RW 140 (100.4,660/34.5,371, 3,646)	Zircon (20)	1.030 (2049)	0.167 (331)	15	6.777 (3,895)	274.4 (-33.1/+37.6)	9.80	1.37 (63)	9.66
RW 141 (100.8,130/34.7,923, 3,454)	Zircon (20)	0.887 (2051)	0.137 (317)	80	6.778 (3,895)	286.5 (-35.0/+39.8)	9.03	1.89 (100)	9.10
RW 162 (97.8,352/34.2,390, 4,747)	Zircon (20)	0.827 (3,335)	0.120 (483)	36	6.778 (3,896)	305.5 (-32.1/+35.7)	9.77	1.17 (100)	9.83
RW 167 (97.2,793/33.0,571, 3,670)	Zircon (20)	0.970 (3,217)	0.166 (552)	9	6.779 (3,896)	258.9 (-26.3/+29.2)	10.54	0.86 (100)	10.58
RW 175 (98.5,067/33.0,128, 4,100)	Zircon (20)	0.778 (3,274)	0.167 (703)	1	6.780 (3,897)	207.8 (-19.9/+21.9)	10.23	1.04 (100)	10.20
RW 181 (96.7,617/33.7,749, 4,126)	Zircon (20)	0.687 (3,729)	0.177 (963)	4.9	6.781 (3,897)	173.3 (-15.3/+16.8)	10.32	1.10 (100)	10.33
RW 182 (96.5,239/33.8,961, 4,064)	Zircon (20)	0.932 (3,457)	0.227 (843)	4.2	6.781 (3,898)	183.3 (-16.8/+18.4)	9.99	1.24 (100)	9.88
RW 188 (94.6,607/34.9,568, 4,415)	Zircon (20)	0.571 (3,144)	0.146 (805)	27	6.782 (3,898)	174.7 (-16.2/+17.9)	9.61	1.40 (100)	9.66
RW 195 (94.2,112/35.6,309, 5,037)	Zircon (20)	0.844 (1973)	0.259 (605)	21	6.783 (3,899)	146.2 (-15.1/+16.8)	10.05	1.30 (75)	10.02
RW 197 (94.2,745/35.7,393, 4,194)	Zircon (20)	0.746 (2065)	0.289 (799)	6	6.784 (3,899)	116.2 (-11.2/+12.4)	9.20	1.37 (100)	9.16

Note: Track densities are ($\times 10^7$ tr/cm²), *=($\times 10^5$ tr/cm²) numbers of tracks counted (N) shown in brackets.

Analysis by external detector method using 0.5 for the $4\pi/2\pi$ geometry correction factor.

Ages calculated using dosimeter glass CN-2 for zircon with $\zeta_{\text{CN2}} = 134 \pm 4$.

$P(\chi^2)$ is probability for obtaining χ^2 value for ν degrees of freedom, where $\nu = \text{no. crystals} - 1$.

Track length data are given in 10^{-6} m, SD = 1σ standard deviation. L_{60} is the mean track length for those confined tracks with an angle $\leq 60^\circ$ to the c-axis (see Yamada et al., 1995, for explanation).

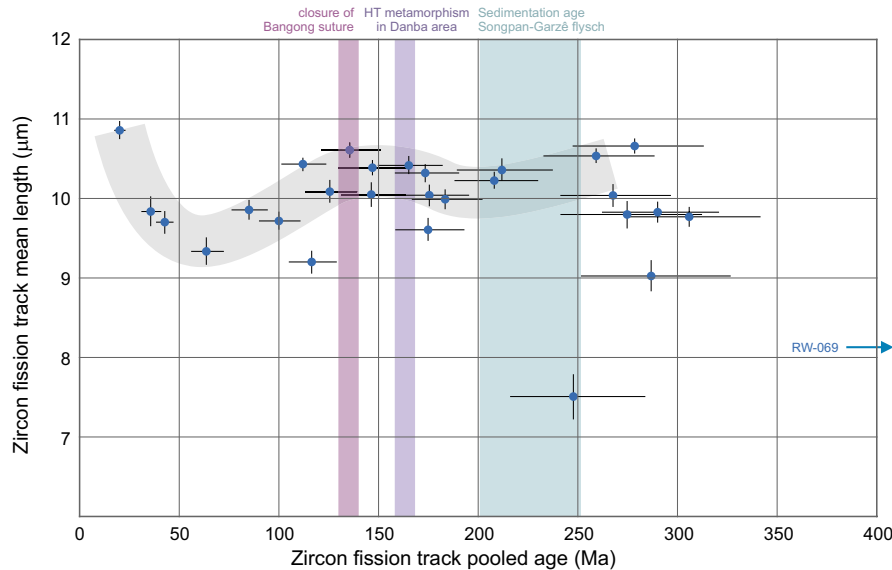


FIGURE 3 Pooled age versus mean track length (boomerang) plot for the zircon samples of the Songpan-Garzê flysch, Tibetan Plateau. A set of two subsequent boomerang relationships is suggested due to a group of intermediate ages between 170 and 110 Ma with relatively long and unimodal track lengths. Coloured time ranges show potential temporal brackets for the burial and exhumation history, related to (with decreasing age) the Triassic sedimentation age of the Songpan-Garzê flysch, geochronological information about the metamorphic overprint in the Danba area (Huang et al., 2003) and the closure of the Bangong suture zone (Zhu et al., 2016)

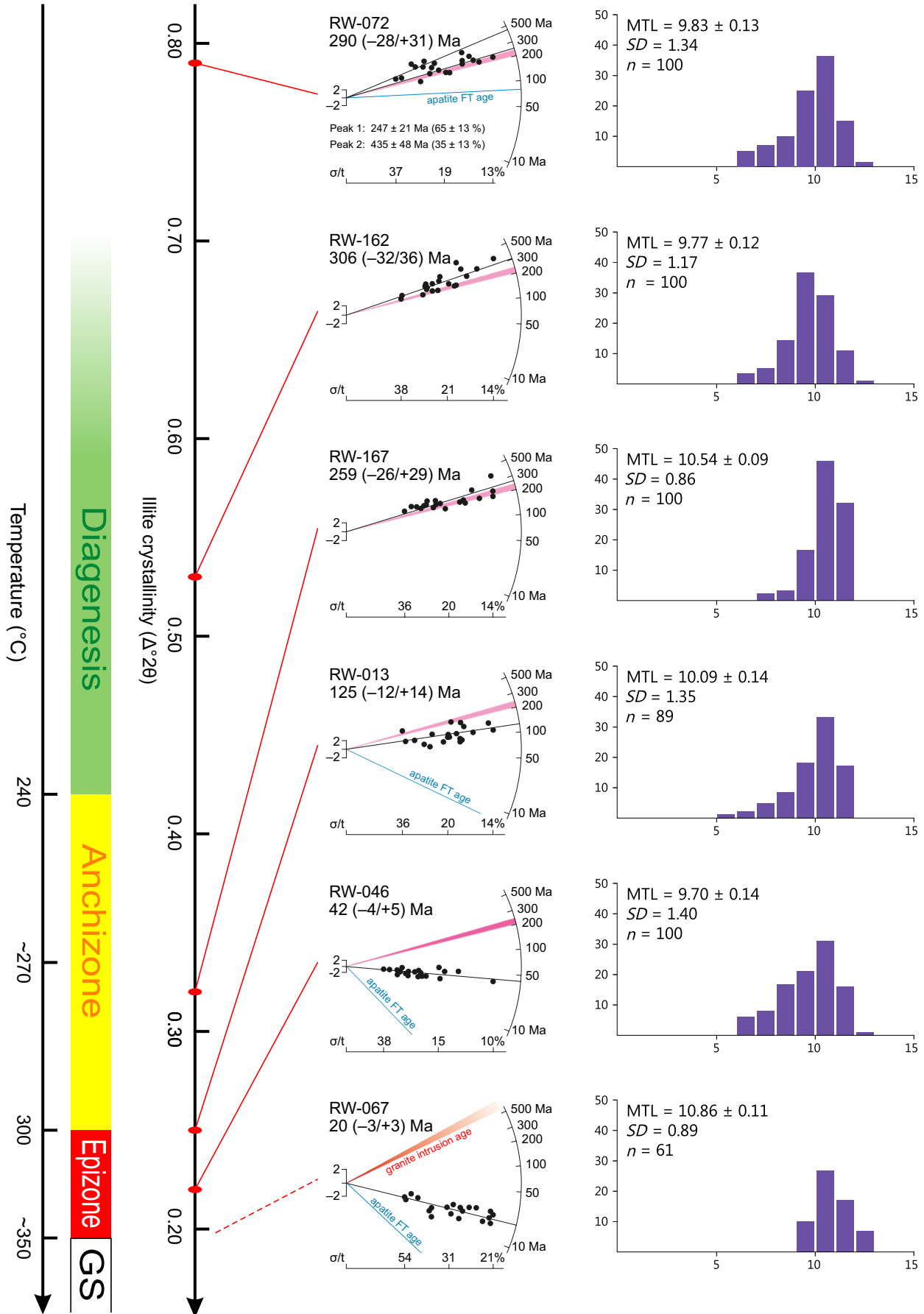
length distribution, and (c) the pass or failure of the χ^2 test (Table 2). We note that part of these aspects contain compulsory arguments (e.g. single grain ages younger than sedimentation age must indicate annealing), while others may only provide supporting evidence (e.g. a failed χ^2 test is not a compulsory argument for annealing, as an initial detrital age distribution may also cause failure). A completely unreset sample may pass the χ^2 test (in case of a relatively homogeneous detrital age signal), may show only long track lengths (in case of a fast cooling hinterland, as expected for this case) and all single grains (within uncertainty) must be older or equal to the sedimentation age. A partially reset sample should fail the χ^2 test, must show shortened track lengths (i.e. a substantial amount of track lengths below 10 μm , leading to a skewed track length distribution and/or a mean track length <10 μm), and at least one single grain age (including its uncertainty) must be younger than the sedimentation age range. Finally, a fully reset zircon FT age should pass the χ^2 test (if age variation is not caused by composition or radiation damage), should only show long track lengths and the mean zircon FT age would be in a time range expected for constant cooling across the partial annealing zones of the zircon and apatite FT systems. Additionally a status of advanced

annealing is defined, if all single grain ages are younger than the sedimentation age range.

According to this evaluation, only a few samples are considered unreset (RW-72, -162 and -167, with IC values ranging from 0.32 to 0.79 $\Delta^{\circ}20$). The majority is assigned a partially annealed status (with IC values ranging from 0.22 to 0.40 $\Delta^{\circ}20$); only one sample (RW-67, greenschist facies overprint) shows full resetting. Advanced annealing is observed for the samples RW-10, -11, -45, -46, -48, -65, and -197 (corresponding to IC values of 0.22–0.24 $\Delta^{\circ}20$). A deviating IC value of 0.40 $\Delta^{\circ}20$ is observed for RW-197. This sample has been taken from a greenschist facies host rock and we suggest that the IC value does not represent maximum temperature conditions.

The temperature range for the lower and upper anchizone boundaries can be estimated based on a comparison of illite crystallinity values with vitrinite reflectance and fluid inclusion homogenization temperatures to be at around 240 and 300°C respectively (Mullis, Ferreiro-Mählmann, & Wolf, 2018). The samples RW-11 and -48 yield epizonal IC values and show the neoformation of biotite (Wang et al., 2008), but these two samples have not undergone full resetting. First evidence for annealing occurs at

FIGURE 4 Representative zircon fission track (FT) samples and their FT data (shown as radial plots, using the programme 'Radial plotter' by Vermeesch, 2009), ordered with increasing illite crystallinity. The two samples to the top (diagenesis) show zircon FT single grain ages in the range or older than the Triassic sedimentation age range (marked in pink). The third sample from top (lower anchizone) has no counted single grain ages statistically younger than the Triassic sedimentation age range, which would prove initial annealing. The fourth sample (anchizone/epizone boundary, ~300°C) shows many single grain ages younger than the sedimentation age, clearly indicating partial annealing. For sample number five (epizone) all single grain ages are significantly younger than the sedimentation age range (advanced annealing), but the zircon FT age is more than 10 times older than the apatite FT age. Only the sample to the bottom (RW-067, Proterozoic granite, which intruded a crustal segment that is distinctly older than the Songpan-Garzê flysch and today shows greenschist facies (GS) overprint) shows full resetting



mid anchizone IC values, suggesting a lower zircon PAZ boundary at around 270°C.

4 | DISCUSSION

According to laboratory-based annealing studies, which cover a time range of 1–10⁷ s (Murakami, Yamada, & Tagami, 2006; Tagami et al., 1998), the temperature range of the zircon partial annealing

zone shows decreasing temperatures with increasing time duration of a thermal event. For the extrapolation of the thermal annealing characteristics to time durations of 10¹³–10¹⁵ s (corresponding to 10⁵–10⁸ a) different potential models (parallel, fanning, curvilinear) have been proposed (e.g. Tagami et al., 1998). Field constraints with tightly defined time and temperature settings are needed to provide information on FT annealing at geological time scales (e.g. Bernet, 2009; Tagami, Carter, & Hurford, 1996). In contrast to laboratory annealing experiments, natural long-term annealing experiments such

TABLE 2 Evaluation of annealing status of 28 zircon samples from the Songpan-Garzê flysch, Tibetan Plateau, China, based on the three aspects age range, track lengths and χ^2 test (subdivided in arguments a–i)

Sample no.	Sed. age	IC ($\Delta^{\circ}2\theta$)	Age range				Track length			χ^2 test		Annealing status
			a	b	c	d	e	f	g	h	i	
RW-10	T2	0.22			■					■		Advanced annealing
RW-11	T2	0.22			■					■		Advanced annealing
RW-13	T3	0.25		■				■			■	Partial annealing
RW-45	T3	0.24			■					■		Advanced annealing
RW-46	T3	0.22			■					■		Advanced annealing
RW-47	T3	0.24		■				■		■		Partial annealing
RW-48	T3	0.24		■			■				■	Advanced annealing
RW-49	T3	0.23		■				■			■	Partial annealing
RW-50	T3	0.37		■						■		Partial annealing
RW-52	T3	0.26		■				■			■	Partial annealing
RW-65	P	0.24			■					■		Advanced annealing
RW-67	late Pr	GF			■	■	■					Full resetting
RW-68	D	^a		■						■	■	Partially annealed
RW-69	D	^a	■							■	■	Partially annealed
RW-72	T3	0.79	■							■	■	No annealing
RW-94	T2-T3	0.37		■				■			■	Partially annealed
RW-127	T2-T3	0.29	■							■		Partially annealed
RW-139	T2-T3	0.27	■								■	Partially annealed
RW-140	T1	0.27		■						■		Partially annealed
RW-141	T1	0.30	■							■		Partially annealed
RW-162	T3	0.53		■						■		No annealing
RW-167	T3	0.32	■							■		No annealing
RW-175	T3	0.26		■						■		Partially annealed
RW-181	T3	0.27		■						■		Partially annealed
RW-182	T2	0.26		■						■	■	Partially annealed
RW-188	T3	0.26		■						■	■	Partially annealed
RW-195	T2	0.27		■						■		Partially annealed
RW-197	C	0.40 ^b		■	■					■		Advanced annealing

Sedimentation age: Pr = Proterozoic (intrusion age), D = Devonian, C = Carboniferous (age of metamorphism) P = Permian, T1 = Lower Triassic, T2 = Middle Triassic, T3 = Upper Triassic, GF = greenschist facies.

Arguments include: (a) single grain ages (including their uncertainty) overlap with or are older than the sedimentation age range, (b) at least one single grain age (including its uncertainty) is younger than the sedimentation age range, (c) all grain ages are younger than the sedimentation age range, (d) the pooled age is approximately double the apatite FT age, (e) track lengths are all long and the length distribution is unimodal, (f) the mean track length is long (>10 μm), but a number of short tracks (<8 μm) leads to a skewed distribution, (g) the mean track length shows shortening (<10 μm), (h) sample passes the χ^2 test (unimodal grain age distribution), (i) sample fails the χ^2 test.

^aNo illite crystallinity (IC) measured.

^bIC value questionable, as sampled rock is a mica schist.

as the data presented in this study may display large differences in initial age and U content, leading to differences in accumulated radiation damage and therefore variable etching and annealing conditions. As a consequence, the annealing status within one individual sample may vary strongly, with some grains annealed at relatively lower temperatures, while others may behave more like zero-damage grains (Rahn et al., 2004), which anneal at higher temperatures.

The amount of accumulated radiation damage within the counted zircon grains during FT annealing is unknown. However, we note that for unreset flysch samples (e.g. RW-162 and -167) the counted grains show a relatively small age scatter (see radial plots in the Data S1). These samples pass the χ^2 test (Tables 1 and 2) and show single grain ages close to or within the sedimentation age range (indicating very short lag times, Bernet & Garver, 2005) due to their origin from the fast exhuming Qinling-Dabie orogen. In order to define the upper zircon PAZ boundary, the focus was set on dating the youngest grains. This may potentially lead to missing the first traces of initial annealing. Therefore, the estimated temperature (mid anchizone, Figure 4) for the first evidence of annealing should be considered a maximum temperature for the lower PAZ boundary.

Previous studies have analysed the temperature range of the zircon fission track partial annealing zone with respect to their sample material and the accumulated radiation damage (Brandon et al., 1998; Rahn et al., 2004). Depending on whether the zircons under investigation are characterized by accumulated radiation damage or not, the partial annealing zone may extend to distinctly different temperatures (Figure 5, Reiners & Brandon, 2006). Field studies on the annealing behaviour in zircon under well-defined geological time and temperature boundary conditions are rare (e.g. Bernet, 2009; Brix et al., 2002; Carter, 1990; Liu, Hsieh, Chen, & Chen, 2001; Tagami & Shimada, 1996; Tagami et al., 1996). Liu et al. (2001) suggested a transition between partially and fully annealed zircons at the transition between prehnite-pumpellyite and greenschist facies. This is in line with this study, as we observe two samples (RW-011 and RW-048) with epizonal IC values, containing new-formed biotite (Wang et al., 2008), but no full resetting of the zircon FT system. In the European Alps, biotite neoformation in metapelitic rocks requires temperatures of $340 \pm 20^\circ\text{C}$ (Nibourel, 2019). Thus, for the zircon FT partial annealing zone in the Songpan-Garzê flysch a temperature window between ~ 270 and 350°C is estimated based on IC values and biotite neoformation. Full resetting requires greenschist facies conditions ($T > 350^\circ\text{C}$).

Results of this study provide an important long-term annealing constraint underlining that even samples that underwent conditions of epizonal illite crystallinity (corresponding to a minimum temperature of 300°C) for 100 myr may still not be fully reset, even though these zircons under investigation may have had the opportunity to gather a large amount of radiation damage during their geological history. Guenther, Reiners, Ketcham, Nasdala, and Giester (2013) suggested that the temperature range for radiation damage annealing corresponds roughly to the zircon FT partial annealing zone. If correct, one would expect that in the case of the anchizone to epizonal Songpan-Garzê flysch and its long-term static thermal evolution (Figure 2), radiation damage would probably form and anneal

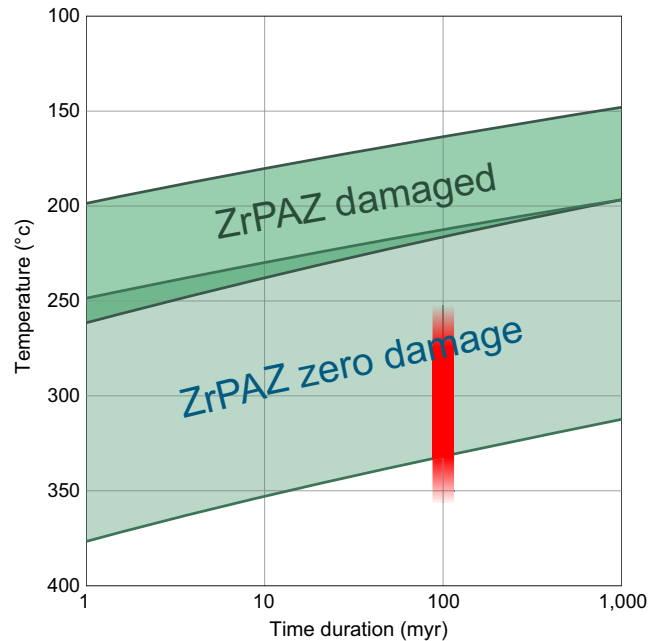


FIGURE 5 Boundary temperatures of the zircon (Zr) partial annealing zone (PAZ) and their relationship from the time duration of a thermal event (from Reiners & Brandon, 2006), depending on the presence or absence of radiation damage. Results of this study show a temperature window of $270\text{--}350^\circ\text{C}$ for track annealing during a time duration of ~ 100 myr. For time duration, see Figure 2, for temperature range, see Figure 4

with similar rate during this period. Accordingly, the zircons would have resided in a continuous state of low radiation damage during FT annealing and not behave like 'damaged' zircons, which would reach full resetting at around 220°C (Reiners & Brandon, 2006; see Figure 5). The temperature range derived in this study extends to the proposed upper limit of the zero-damage partial annealing zone (at $\sim 330^\circ\text{C}$), because the zircon grains with slowest etching anneal similar to 'zero-damage' zircons.

The Guenther et al. (2013)'s zircon radiation damage accumulation and annealing model was criticised recently for not being fully correct (e.g. Anderson, Hodges, & van Soest, 2017; Mackintosh, Kohn, Gleadow, & Tian, 2017). Furthermore, Ginster et al. (2019) and Jonckheere et al. (2019) have demonstrated that radiation damage is a complex pattern of different sorts of damage annealing over a large temperature range. Thus, the results of this study only refer to the radiation damage that influences FT annealing.

5 | CONCLUSIONS

For the Songpan-Garzê flysch, a thermal overprint lasting for ~ 100 myr has led to a range of unreset to completely reset zircon FT ages. A metamorphic window of upper anchizone to epizonal illite crystallinity values, corresponding to a temperature range of $270\text{--}350^\circ\text{C}$, shows evidence of partial FT annealing. Time and

temperature ranges extend well into proposed partial annealing zone for zero-damage zircons. It is suggested that the annealing behaviour in a zero-damage setting is due to the continuous annealing of the relevant radiation damage during FT annealing over long time duration.

A save strategy to ensure obtaining fully reset and therefore cooling zircon FT ages within orogenic belts is to restrict sampling to areas that have undergone in minimum greenschist facies conditions ($\geq 350^\circ\text{C}$), even if the thermal plateau has endured for long time durations. For studies using detrital zircon FT information, ages representing the exhumation signal of the hinterland can only be expected from areas with greenschist facies overprint, while areas of only diagenetic to lower anchizonal overprint ($\leq 270^\circ\text{C}$) are likely to still contain the original detrital (pre-metamorphic) time information.

ACKNOWLEDGEMENTS

This study was supported by the National Natural Science Foundation of China (grants no. 40972038, 40572032 and 40872034). We owe our thanks to A. Wetzel and A. Kounov for access to the Basel mineral separation facilities and fission track laboratory. The manuscript has substantially profited from thorough assessments by M. Bernet and two anonymous reviewers.

ORCID

Meinert Rahn  <https://orcid.org/0000-0003-2321-7248>

REFERENCES

- Anderson, A. J., Hodges, K. V., & van Soest, M. C. (2017). Empirical constraints on the effects of radiation damage on helium diffusion in zircon. *Geochimica et Cosmochimica Acta*, 218, 308–322.
- Bernet, M. (2009). A field-based estimate of the zircon fission-track closure temperature. *Chemical Geology*, 259, 181–189. <https://doi.org/10.1016/j.chemgeo.2008.10.043>
- Bernet, M., & Garver, J. I. (2005). Fission-track analysis of detrital zircon. In P. W. Reiners & T. A. Ehlers (Eds.), *Low-temperature thermochronology* (pp. 205–238). *Reviews in Mineralogy and Geochemistry*, 58. <https://doi.org/10.1515/9781501509575>
- Brandon, M. T., Roden-Tice, M. K., & Garver, J. I. (1998). Late Cenozoic exhumation of the Cascadia accretionary wedge in the Olympic Mountains, northwest Washington State. *Geological Society of America Bulletin*, 110, 985–1009. [https://doi.org/10.1130/0016-7606\(1998\)110<0985:LCEOTC>2.3.CO;2](https://doi.org/10.1130/0016-7606(1998)110<0985:LCEOTC>2.3.CO;2)
- Brix, M. R., Stöckhert, B., Seidel, E., Theye, T., Thomson, S. N., & Kuster, M. (2002). Thermobarometric data from a fossil zircon partial annealing zone in high pressure-low temperature rocks of eastern and central Crete, Greece. *Tectonophysics*, 349, 309–326. [https://doi.org/10.1016/S0040-1951\(02\)00059-8](https://doi.org/10.1016/S0040-1951(02)00059-8)
- Carter, A. (1990). The thermal history and annealing effects in zircons from the Ordovician of North Wales. *Nuclear Tracks Radiation Measurements*, 17, 309–313. [https://doi.org/10.1016/1359-0189\(90\)90051-X](https://doi.org/10.1016/1359-0189(90)90051-X)
- Chen, W., & Arnaud, N. (1997). Isotope geochronology study for 'POG type' granite in Bayan Har Terrane, Qinghai-Xizang Plateau, China (in Chinese, with English abstract). *Acta Geoscientia Sinica*, 18, 261–266.
- Fleischer, R. L., Price, P. B., & Walker, R. M. (1965). Effects of temperature, pressure and ionization on the formation and stability of fission tracks in minerals and glasses. *Journal of Geophysical Research*, 70, 1497–1502. <https://doi.org/10.1029/JZ070i006p01497>
- Garver, J. I., & Kamp, P. J. J. (2002). Integration of zircon color and zircon fission-track zonation patterns in orogenic belts: application to the Southern Alps, New England. *Tectonophysics*, 349, 203–219.
- Ginster, U., Reiners, P. W., Nasdala, L., & Chanmuang, N. C. (2019). Annealing kinetics of radiation damage in zircon. *Geochimica et Cosmochimica Acta*, 249, 225–246. <https://doi.org/10.1016/j.gca.2019.01.033>
- Gleadow, A. J. W., Hurford, A. J., & Quaife, R. D. (1976). Fission track dating of zircon: Improved etching techniques. *Earth and Planetary Science Letters*, 33, 273–276. [https://doi.org/10.1016/0012-821X\(76\)90235-1](https://doi.org/10.1016/0012-821X(76)90235-1)
- Guenther, W. R., Reiners, P. W., Ketcham, R. A., Nasdala, L., & Giester, G. (2013). Helium diffusion in natural zircon: Radiation damage, anisotropy, and the interpretation of zircon (U-Th)/He thermochronology. *American Journal of Science*, 313, 145–198. <https://doi.org/10.2475/03.2013.01>
- Guenther, W. R., Reiners, P. W., & Tian, Y. (2014). Interpreting data-eU correlations in zircon (U-Th)/He datasets: A case study from the Longmen Shan, China. *Earth and Planetary Science Letters*, 403, 328–339. <https://doi.org/10.1016/j.epsl.2014.06.050>
- Hu, J., Meng, Q., Shi, Y., & Qu, H. (2005). SHRIMP U-Pb dating of zircons from granitoid bodies in the Songpan-Ganzi terrane and its implications. *Acta Petrologica Sinica*, 21, 867–880.
- Huang, M., Maas, R., Buick, I. S., & Williams, I. S. (2003). Crustal response to continental collisions between the Tibet, Indian, South China and North China blocks: Geochronological constraints from the Songpan-Garzê orogenic belt, western China. *Journal of Metamorphic Geology*, 21, 223–240. <https://doi.org/10.1046/j.1525-1314.2003.00438.x>
- Jonckheere, R., Heinz, D., Hacker, B., Rafaja, D., & Ratschbacher, L. (2019). A borehole investigation of zircon radiation damage. *Terra Nova*, 31, 263–270.
- Kasuya, M., & Naeser, C. W. (1988). The effect of α -damage on fission-track annealing in zircon. *Nuclear Tracks*, 14, 477–480. [https://doi.org/10.1016/1359-0189\(88\)90008-8](https://doi.org/10.1016/1359-0189(88)90008-8)
- Kirby, E., Reiners, P. W., Krol, M. A., Whipple, K. X., Hodges, K. V., Farley, K. A., ... Chen, Z. (2002). Late Cenozoic evolution of the eastern margin of the Tibetan Plateau: Inferences from $^{40}\text{Ar}/^{39}\text{Ar}$ and (U-Th)/He thermochronology. *Tectonics*, 21, 3–22.
- Krishnaswami, S., Lal, D., Prabhu, N., & MacDougall, D. (1974). Characteristics of fission tracks in zircon: Applications to geochronology and cosmology. *Earth and Planetary Science Letters*, 22, 51–59. [https://doi.org/10.1016/0012-821X\(74\)90063-6](https://doi.org/10.1016/0012-821X(74)90063-6)
- Laslett, G. M., Kendall, W. S., Gleadow, A. J. W., & Duddy, I. R. (1982). Bias in measurement of fission-track length distributions. *Nuclear Tracks and Radiation Measurements*, 6, 79–85. [https://doi.org/10.1016/0735-245X\(82\)90031-X](https://doi.org/10.1016/0735-245X(82)90031-X)
- Liu, T., Hsieh, S., Chen, Y., & Chen, W. (2001). Thermo-kinematic evolution of the Taiwan oblique-collision mountain belt as revealed by zircon fission track dating. *Earth and Planetary Science Letters*, 186, 45–56. [https://doi.org/10.1016/S0012-821X\(01\)00232-1](https://doi.org/10.1016/S0012-821X(01)00232-1)
- Ma, Y., Fu, X., Wu, J., & Chen, G. (2007). Crustal structural and tectonic evolution and oil prospect evaluation in the Songpan-Zoige Block. *Acta Geologica Sinica (English Edition)*, 81, 55–60.
- Ma, Y., Mou, C., Guo, X., Yu, Q., & Tan, Q. (2006). Sedimentary facies and distribution of reservoir rocks from the Feixianguan Formation in the Daxian-Xuanhan region, NE Sichuan. *Acta Geologica Sinica (English Edition)*, 80, 137–151.
- Mackintosh, V., Kohn, B., Gleadow, A., & Tian, Y. (2017). Phanerozoic morphotectonic evolution of the Zimbabwe Craton: Unexpected outcomes from a multiple low-temperature thermochronology

- study. *Tectonics*, 36, 2044–2067. <https://doi.org/10.1002/2017T C004703>
- Mullis, J., Ferreiro-Mählmann, R., & Wolf, M. (2018). Fluid inclusion microthermometry to calibrate vitrinite reflectance (between 50 and 270°C), illite Kübler-Index data and the diagenesis/anchizone boundary in the external part of the Central Alps. *Applied Clay Science*, 143, 307–319.
- Murakami, M., Yamada, R., & Tagami, T. (2006). Short-term annealing characteristics of spontaneous fission tracks in zircon: A qualitative description. *Chemical Geology*, 227, 214–222. <https://doi.org/10.1016/j.chemgeo.2005.10.002>
- Nibourel, L. (2019). The structural and thermo-kinematic evolution of the eastern Aar Massif, Switzerland. Unpubl. PhD thesis, University of Berne, 137 pp.
- Pullen, A., Kapp, P., Gehrels, G., Vervoot, J. D., & Ding, L. (2008). Triassic continental subduction in central Tibet and Mediterranean-style closure of the Paleo-Tethys Ocean. *Geology*, 36, 351–354. <https://doi.org/10.1130/G24435A.1>
- Rahn, M. K., Brandon, M. T., Batt, G. E., & Garver, J. I. (2004). A zero-damage model for fission-track annealing in zircon. *American Mineralogist*, 89, 473–484. <https://doi.org/10.2138/am-2004-0401>
- Reiners, P. W., & Brandon, M. T. (2006). Using thermochronology to understand orogenic erosion. *Annual Review on Earth and Planetary Sciences*, 34, 419–466. <https://doi.org/10.1146/annurev.earth.34.031405.125202>
- Roger, F., Jolivet, M., Cattin, R., & Malavieille, J. (2011). Mesozoic-Cenozoic tectonothermal evolution of the eastern part of the Tibetan Plateau (Songpan-Garzê, Longmen Shan area): Insights from thermochronological data and simple thermal modelling. *Geological Society of London Special Publications*, 353, 9–25. <https://doi.org/10.1144/SP353.2>
- Roger, F., Malavieille, J., Leloup, P. H., Calassou, S., & Xu, Z. (2004). Timing of granite emplacement and cooling in the Songpan-Garzê fold belt (eastern Tibetan Plateau) with tectonic implications. *Journal of Asian Earth Sciences*, 22, 465–481. [https://doi.org/10.1016/S1367-9120\(03\)00089-0](https://doi.org/10.1016/S1367-9120(03)00089-0)
- Tagami, T., Carter, A., & Hurford, A. J. (1996). Natural long-term annealing of the zircon fission-track system in Vienna Basin deep borehole samples: Constraints upon the partial annealing zone and closure temperature. *Chemical Geology*, 130, 147–157. [https://doi.org/10.1016/0009-2541\(96\)00016-2](https://doi.org/10.1016/0009-2541(96)00016-2)
- Tagami, T., Galbraith, R. F., Yamada, R., & Laslett, G. M. (1998). Revised annealing kinetics of fission tracks in zircon and geological implications. In P. van den Haute & F. De Corte (Eds.), *Advances in fission-track geochronology* (pp. 99–112). Dordrecht, The Netherlands: Kluwer. <https://doi.org/10.1007/978-94-015-9133-1>
- Tagami, T., & Shimada, C. (1996). Natural long-term annealing of the zircon fission-track system around a granitic pluton. *Journal of Geophysical Research*, 101, 8245–8255. <https://doi.org/10.1029/95JB02885>
- Vermeesch, P. (2009). RadialPlotter: A Java application for fission track, luminescence and other radial plots. *Radiation Measurements*, 44, 409–410. <https://doi.org/10.1016/j.radmeas.2009.05.003>
- Wang, G., Cao, K., Zhang, K., Wang, A., Liu, C., Meng, Y., & Xu, Y. (2011). Spatio-temporal framework of tectonic uplift stages of the Tibetan Plateau in Cenozoic. *Science China Earth Sciences*, 54, 29–44. <https://doi.org/10.1007/s11430-010-4110-0>
- Wang, G., Wintsch, R. P., Garver, J. I., Roden-Tice, M., Chen, S., Zhang, K., ... Li, D. (2009). Provenance and thermal history of the Bayan Har Group in the western-central Songpan-Ganzi-Bayan Har terrane: Implications for tectonic evolution of the northern Tibetan Plateau. *Island Arc*, 18, 444–466. <https://doi.org/10.1111/j.1440-1738.2009.00666.x>
- Wang, H., Ma, Y., Zhou, J., & Xu, T. (2012). Diagenesis and very low grade metamorphism in a 7,012 m-deep well Hongcan 1, eastern Tibetan plateau. *Swiss Journal of Geosciences*, 105, 249–261. <https://doi.org/10.1007/s00015-012-0105-5>
- Wang, H., Rahn, M., Tao, X., Zheng, N., & Xu, T. (2008). Diagenesis and metamorphism of Triassic Flysch along profile Zoigê-Lushan, north-west Sichuan, China. *Acta Geologica Sinica*, 82, 917–926.
- Wang, H., Rahn, M., & Zhou, J. (2018). Tectonothermal evolution of the Triassic flysch in the Bayan Har Orogen, Tibetan plateau. *Tectonophysics*, 723, 277–287. <https://doi.org/10.1016/j.tecto.2017.12.020>
- Wang, H., Rahn, M., Zhou, J., & Tao, X. (2013). Tectonothermal evolution of the Triassic flysch in the Songpan-Garzê orogen, eastern Tibetan plateau. *Tectonophysics*, 608, 505–516. <https://doi.org/10.1016/j.tecto.2013.08.036>
- Warr, L. N., & Rice, A. H. N. (1994). Interlaboratory standardization and calibration of day mineral crystallinity and crystallite size data. *Journal of Metamorphic Geology*, 12, 141–152. <https://doi.org/10.1111/j.1525-1314.1994.tb00010.x>
- Weislogel, A. L., Graham, S. A., Chang, E. Z., Wooden, J. L., Gehrels, G. E., & Yang, H. (2006). Detrital zircon provenance of the Late Triassic Songpan-Ganzi complex: Sedimentary record of collision of the North and South China blocks. *Geology*, 34, 97–100. <https://doi.org/10.1130/G21929.1>
- Yamada, R., Tagami, T., Nishimura, S., & Ito, H. (1995). Annealing kinetics of fission tracks in zircon: An experimental study. *Chemical Geology*, 122, 249–258. [https://doi.org/10.1016/0009-2541\(95\)00006-8](https://doi.org/10.1016/0009-2541(95)00006-8)
- Zhu, D., Li, S., Cawood, P. A., Wang, Q., Zhao, Z., Liu, S., & Wang, L. (2016). Assembly of the Lhasa and Qiangtang terranes in central Tibet by divergent double subduction. *Lithos*, 245, 7–17. <https://doi.org/10.1016/j.lithos.2015.06.023>

SUPPORTING INFORMATION

Additional supporting information may be found online in the Supporting Information section at the end of the article.

Data S1. This supplementary data file contains (a) radial plots, track length histograms, age-U content diagrams for all 28 samples of this study, (b) a table showing the etching conditions for each of the samples and sample mounts, (c) a methodical description of the IC measurements, which form the basis of the temperature estimations for partial and total annealing.

How to cite this article: Rahn M, Wang H, Dunkl I. A natural long-term annealing experiment for the zircon fission track system in the Songpan-Garzê flysch, China. *Terra Nova*. 2019;00:1–11. <https://doi.org/10.1111/ter.12399>